Emission properties of an oscillating point dipole from a gold Yagi-Uda nanoantenna array

S. V. Lobanov,[1,2] T. Weiss,[3] D. Dregely,[3] H. Giessen,[3] N. A. Gippius,[2,4] and S. G. Tikhodeev[1,2]
[1]*M. V. Lomonosov Moscow State University, Leninskie Gory 1, Moscow 119991, Russia*
[2]*A. M. Prokhorov General Physics Institute, Russian Academy of Sciences, Vavilova Street 38, Moscow 119991, Russia*
[3]*4th Physics Institute and Research Centers Scope and Simtech, University of Stuttgart, D-70550 Stuttgart, Germany*
[4]*LASMEA, University Blaise Pascal, 24 Avenue des Landais, F-63177 Aubière Cedex, France*
(Received 11 September 2011; revised manuscript received 10 March 2012; published 24 April 2012)

We investigate numerically the interaction of an oscillating point dipole with a periodic array of optical Yagi-Uda nanoantennas in the weak coupling limit. A very strong near-field enhancement of the dipole emission by the resonant plasmon mode in the feed element is predicted in this structure. It is shown that the enhancement factor depends strongly on the dipole position, the direction of the dipole moment, and the oscillation frequency. The radiative intensity of the point dipole from appropriate places next to one feed element may exceed the radiative intensity of an equivalent dipole in free-space by a factor of 100. Despite the fact that only one director is used in each nanoantenna of the array, the far-field emission pattern is highly directed. The radiative efficiency (the ratio of the radiative to the total emission) is around 20%.

DOI: 10.1103/PhysRevB.85.155137 PACS number(s): 78.67.Lt, 42.60.Da, 73.20.Mf, 78.67.Hc

I. INTRODUCTION

Nanophotonics has been the focus of intensive investigations in recent years. One of its numerous areas is the nanoscale control of light emission from a single molecule or quantum dot. Promising tools for the realization of this goal are optical nanoantennas.[1–14]

Metal antennas are traditionally used for controlling the radiation pattern of electromagnetic wave emission in the radio and microwave frequency range. Though the electromagnetic properties of metals in the optical range differ significantly from that in the radio and microwave range, it seems to be reasonable to use the main concepts of radio antennas in the optical range as well. It has been suggested[1–6] to construct a nanooptical antenna with elements that are arranged as in the radio Yagi-Uda antennas.

Yagi-Uda antennas consist usually of one or two reflectors, one feed element and several directors with appropriately selected scattering phases (reflector and director are slightly detuned inductively and capacitively). As has been recently shown, the nanoantenna elements can be nanorods,[2–4] core-shell,[1,5] or spherical[14] nanoparticles. All elements scatter the light, and the resulting interference forms a highly directed beam along the antenna axis. The size of the elements in such optical Yagi-Uda nanoantennas has to be smaller than the light emission wavelength in free-space. Such optical nanoantennas only work efficiently in narrow frequency domains, where the interaction of the emitter with light is resonantly enhanced because of the excitation of localized plasmons[15,16] in the nanoantenna elements.

Spontaneous emission is not an intrinsic atomic property but depends sensitively on the local density of photonic modes at certain frequencies in a microcavity,[17,18] or, equivalently, on the local electromagnetic field value at the position of the quantum emitter.[8,9,13] Using resonances, it is possible to increase the local electromagnetic field significantly, and, consequently, to enhance and redirect the dipole emission. In the case of localized plasmon resonances, the collective excitation of electrons at the plasmon frequency leads to a considerably enhanced emission rate when the point dipole is located in the vicinity of metallic nanoparticles with the appropriate orientation of its dipole moment.[3,10,12]

The exact description of photon radiation from the quantum emitter located in some metal-dielectric environment is very complicated. A convenient approximation is the model of an oscillating point dipole. It oscillates with constant frequency and magnitude fixed by the external source (so-called weak coupling limit). In other words, the emission of a current $\vec{j}(\vec{r},t) = \vec{j}_0 \cdot \delta(\vec{r} - \vec{r}_0) \cdot e^{-i\omega t}$ inside an environment with spatially modulated permittivity has to be calculated. This system is now classical and can be described by Maxwell's equations.

The goal of this paper is to investigate the radiation pattern and emission rate of one oscillating point dipole located in a periodic array of optical Yagi-Uda nanoantennas. Each antenna in the array consists of three rectangular gold elements: director, feed, and reflector. The point emitter is located a few nanometers from the edge of one feed element. To the best of our knowledge, the emission properties of an oscillating point dipole from such a structure have not been investigated yet. The structures investigated so far have been either single Yagi-Uda nanoantennas[1–5] or arrays of simpler spherical shapes.[10] Using arrays of antennas in combination with several emitters with controlled phase difference of oscillation, we would be able to control the optical emission directivity,[19] just like in phased antenna arrays.

The paper is organized as follows. In Sec. II, the Purcell factor and radiative efficiency of an oscillating point dipole inside the nanoantenna array are introduced. The scattering matrix approach is applied for calculation of these quantities. The calculated results for a periodic array of optical Yagi-Uda nanoantennas with an oscillating point dipole are presented in Sec. III. In this section, the calculated spectra, far-field directional pattern of emission, Purcell factor, and radiative efficiency are given and discussed. The results are summarized in Sec. IV.

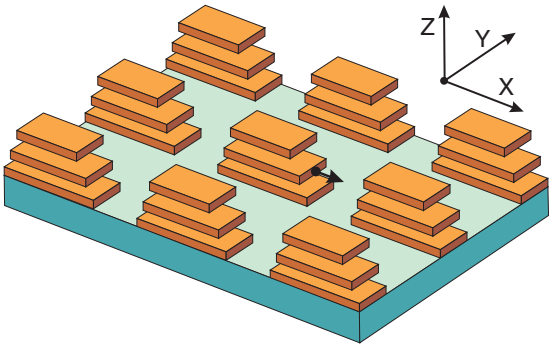

FIG. 1. (Color online) Lateral view of a periodic array of optical Yagi-Uda nanoantennas with an x-oriented oscillating point dipole (black point with arrow) located at a horizontal distance of 5 nm from the feed element of one nanoantenna.

II. SCATTERING MATRIX METHOD FOR EMISSION PROPERTIES CALCULATION

The structure of interest is shown schematically in Fig. 1. It consists of a glass superstrate ($\varepsilon = 2.4$), a periodic array of optical Yagi-Uda nanoantennas that are arranged in a rectangular lattice, and a quartz substrate ($\varepsilon = 2.13$). The periods along the x and y axis are equal to 450 and 300 nm, respectively. Each antenna consists of three rectangular gold parallelepipeds of 30 nm height and 100 nm width. The lengths of the top (director), middle (feed), and bottom (reflector) elements are 220, 250, and 300 nm, respectively. They are located in glass and the vertical distance between them is equal to 100 nm. We assumed the gold permittivity to be described by the Drude formula with 9016 meV plasma frequency and 81 meV damping rate.

Our first goal is to calculate the directional pattern as well as the emission spectra in the direction normal to the antenna plane. It makes sense to normalize the computed emission intensity $P(\vartheta,\varphi)$, i.e., the Poynting vector of the dipole emission in the far field as a function of the spherical angles ϑ and ϕ, to the maximum intensity of the emission of a point dipole in free space, which oscillates with the same magnitude and frequency. Thus, we can easily distinguish the enhancement of emission ($P > 1$) from the attenuation ($P < 1$) compared to the dipole located in homogeneous vacuum.

To characterize quantitatively the total dipole emission and its radiative part, it is convenient to define the Purcell factor and its radiative part as

$$F_{\mathrm{P}} = \frac{\iint_{\Sigma_0}(\vec{P}\cdot d\vec{A})}{\iint_{\Sigma_0}(\vec{P}_0\cdot d\vec{A})}, \quad \text{and} \quad F_{\mathrm{P}}^{\mathrm{rad}} = \frac{\iint_{\Sigma}(\vec{P}\cdot d\vec{A})}{\iint_{\Sigma_0}(\vec{P}_0\cdot d\vec{A})}, \tag{1}$$

respectively. Here, Σ_0 and Σ consist of two horizontal xy planes: in case of Σ_0 infinitesimally below and above the point emitter, in case of Σ below and above the whole nanostructure, i.e., in the substrate and superstrate. $\vec{P}$ is the Poynting vector of the dipole emission from the antenna array, $\vec{P}_0$ is its counterpart for dipole emission in free space. The antenna absorption losses can be characterized by the nonradiative part of the Purcell factor $F_{\mathrm{P}}^{\mathrm{nr}}$,

$$F_{\mathrm{P}}^{\mathrm{nr}} = F_{\mathrm{P}} - F_{\mathrm{P}}^{\mathrm{rad}}. \tag{2}$$

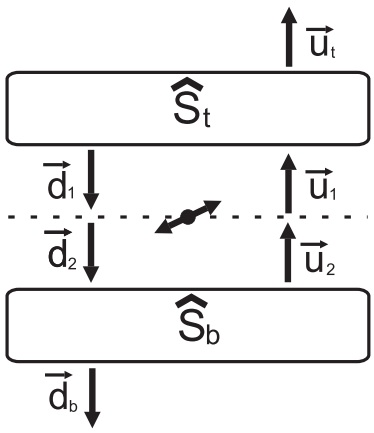

FIG. 2. S-matrix diagram for an oscillating point dipole emission configuration. The rounded rectangles denote the scattering matrices of the top and the bottom laminated structures (see explanation in the text). Vectors $\vec{d}$,$\vec{u}$ with arrows specify amplitudes and the direction of propagation. Amplitudes $\vec{d}_t$ and $\vec{u}_b$ are not shown since they are equal to zero in the considered problem. The central dot with arrows indicates the dipole moment.

Now, we can also introduce the radiative efficiency η, indicating the radiative part of dipole emission,

$$\eta = \frac{F_{\mathrm{P}}^{\mathrm{rad}}}{F_{\mathrm{P}}}. \tag{3}$$

The calculation of the radiation characteristics from oscillating dipoles in two-dimensional photonic crystal slabs can be performed using the scattering matrix approach.[20–22] The basic idea of the method is shown schematically in Fig. 2. First, the system is split by a horizontal xy plane (the dashed horizontal line in that figure) containing the point dipole into two parts above and below the dipole. Then, the top and the bottom partial scattering matrices ($\hat{S}_t$ and $\hat{S}_b$, respectively) are computed and the amplitudes in four principal layers are connected with each other:

$$\begin{pmatrix}\vec{d}_1\\ \vec{u}_t\end{pmatrix} = \begin{pmatrix}\hat{S}_t^{dd} & \hat{S}_t^{du}\\ \hat{S}_t^{ud} & \hat{S}_t^{uu}\end{pmatrix}\begin{pmatrix}\vec{0}\\ \vec{u}_1\end{pmatrix},$$
$$\begin{pmatrix}\vec{d}_b\\ \vec{u}_2\end{pmatrix} = \begin{pmatrix}\hat{S}_b^{dd} & \hat{S}_b^{du}\\ \hat{S}_b^{ud} & \hat{S}_b^{uu}\end{pmatrix}\begin{pmatrix}\vec{d}_2\\ \vec{0}\end{pmatrix}. \tag{4}$$

Note that in these equations amplitudes $\vec{d}_t$ and $\vec{u}_b$ are replaced by zero vectors, which means that external light propagating toward the photonic crystal slab is absent. We rewrite these equations in a slightly different form:

$$\vec{d}_b = \hat{S}_b^{dd}\vec{d}_2, \quad \vec{u}_t = \hat{S}_t^{uu}\vec{u}_1; \tag{5}$$

$$\vec{d}_1 = \hat{S}_t^{du}\vec{u}_1, \quad \vec{u}_2 = \hat{S}_b^{ud}\vec{d}_2. \tag{6}$$

Amplitudes $\vec{d}_n$ and $\vec{u}_n$ ($n = 1,2$) define the electromagnetic field distribution in two horizontal planes (infinitesimally above and below the dipole) via the material

matrix $\hat{F}_n$[23]:

$$\begin{pmatrix} \vec{E}_1 \\ \vec{H}_1 \end{pmatrix} = \hat{F}_1 \begin{pmatrix} \vec{d}_1 \\ \vec{u}_1 \end{pmatrix}, \quad \begin{pmatrix} \vec{E}_2 \\ \vec{H}_2 \end{pmatrix} = \hat{F}_2 \begin{pmatrix} \vec{d}_2 \\ \vec{u}_2 \end{pmatrix}. \tag{7}$$

Here, the electric $\vec{E}$ and magnetic $\vec{H}$ supervectors consist of x and y projections only, i.e., $\vec{E} = (E_x, E_y)^T$, $\vec{H} = (H_x, H_y)^T$. For the sake of simplicity, we assume that the dipole does not lie at the boundary between two different layers, i.e., $\hat{F}_1 = \hat{F}_2 \equiv \hat{F}$ (a solution for the general case will be published elsewhere). In what follows we will need also the general form of a material matrix and its inverse operator (which is valid only for specific symmetric cases[24])

$$\hat{F} = \begin{pmatrix} \hat{E} & \hat{E} \\ \hat{H} & -\hat{H} \end{pmatrix}, \quad \hat{F}^{-1} = \frac{1}{2} \begin{pmatrix} \hat{E}^{-1} & \hat{H}^{-1} \\ \hat{E}^{-1} & -\hat{H}^{-1} \end{pmatrix}. \tag{8}$$

It is straightforward to obtain directly from Maxwell's equations[20,22] that the horizontal components of electric and magnetic fields exhibit discontinuities near the dipole's plane, i.e.,

$$\begin{pmatrix} \vec{E}_2 \\ \vec{H}_2 \end{pmatrix} - \begin{pmatrix} \vec{E}_1 \\ \vec{H}_1 \end{pmatrix} = \begin{pmatrix} \vec{J}_E \\ \vec{J}_H \end{pmatrix}, \tag{9}$$

where

$$\vec{J}_E \equiv -\frac{4\pi}{\omega} \begin{pmatrix} \hat{k}_x \\ \hat{k}_y \end{pmatrix} \hat{\varepsilon}_z^{-1} j_z, \quad \vec{J}_H \equiv \frac{4\pi}{c} \begin{pmatrix} j_y \\ -j_x \end{pmatrix}. \tag{10}$$

In these formulas, c is the speed of light, $\hat{k}_x$ and $\hat{k}_y$ are the differential (momentum) operators, $\hat{\varepsilon}_z^{-1}$ signifies the inverse permittivity z-component operator in momentum space, j_x, j_y, and j_z are the three dipole's current projections in the momentum space. We substitute Eq. (7) to Eq. (9) and multiply it by the inverse material matrix $\hat{F}^{-1}$ using Eqs. (8):

$$\vec{d}_2 - \vec{d}_1 = \vec{J}_d, \tag{11}$$

$$\vec{u}_2 - \vec{u}_1 = \vec{J}_u. \tag{12}$$

Here, we introduced new quantities for brevity,

$$\vec{J}_d = \tfrac{1}{2}(\hat{E}^{-1}\vec{J}_E + \hat{H}^{-1}\vec{J}_H), \quad \vec{J}_u = \tfrac{1}{2}(\hat{E}^{-1}\vec{J}_E - \hat{H}^{-1}\vec{J}_H). \tag{13}$$

We can replace amplitudes $\vec{d}_1$ and $\vec{u}_2$ in Eqs. (11) and (12) by Eqs. (6):

$$\vec{d}_2 - \hat{S}_t^{du}\vec{u}_1 = \vec{J}_d, \tag{14}$$

$$\hat{S}_b^{ud}\vec{d}_2 - \vec{u}_1 = \vec{J}_u. \tag{15}$$

After multiplying Eq. (15) by $-\hat{S}_t^{du}$ and adding it to Eq. (14), we come to an equation for the amplitude $\vec{d}_2$. Similarly, we can derive the amplitude $\vec{u}_1$. Thus,

$$(\hat{1} - \hat{S}_t^{du}\hat{S}_b^{ud})\vec{d}_2 = (\vec{J}_d - \hat{S}_t^{du}\vec{J}_u), \tag{16}$$

$$(\hat{1} - \hat{S}_b^{ud}\hat{S}_t^{du})\vec{u}_1 = (\hat{S}_b^{ud}\vec{J}_d - \vec{J}_u). \tag{17}$$

Finally, one can express amplitudes $\vec{d}_2, \vec{u}_1$ from these equations and obtain the solution of the emission problem,

$$\vec{d}_2 = (\hat{1} - \hat{S}_t^{du}\hat{S}_b^{ud})^{-1}(\vec{J}_d - \hat{S}_t^{du}\vec{J}_u), \tag{18}$$

$$\vec{u}_1 = (\hat{1} - \hat{S}_b^{ud}\hat{S}_t^{du})^{-1}(\hat{S}_b^{ud}\vec{J}_d - \vec{J}_u). \tag{19}$$

Using this solution and Eqs. (6) and (7), one can compute the electromagnetic field distribution in two planes located infinitesimally above and below the dipole. Hence, the power flow through each plane $z = z_{\text{dipole}\pm 0}$ can be calculated as

$$P = \frac{c}{8\pi}\mathrm{Re}(\langle E_x|H_y\rangle - \langle E_y|H_x\rangle). \tag{20}$$

In this case, the scalar product does not depend on the representation and can be calculated in coordinate space

$$\langle E_\alpha|H_\beta\rangle = \int_{-\infty}^{\infty} \mathrm{d}x \int_{-\infty}^{\infty} \mathrm{d}y\, E_\alpha^*(x,y,z)H_\beta(x,y,z), \tag{21}$$

as well as in momentum space

$$\langle E_\alpha|H_\beta\rangle = \int_{-\infty}^{\infty} \mathrm{d}k_x \int_{-\infty}^{\infty} \mathrm{d}k_y\, E_\alpha^*\{k_x,k_y,z\}H_\beta\{k_x,k_y,z\}. \tag{22}$$

Here $\alpha,\beta = x,y$ and * denotes the complex conjugate.

Finally, the total radiative rate can be computed as a difference between the power flow through the upper and lower horizontal planes infinitesimally close to the point dipole:

$$R = P_+ - P_-. \tag{23}$$

In this equation, the minus sign appears because the outward normal to the lower plane is directed oppositely to the z axis. Strictly speaking, the total radiative rate is by definition the power flow through an infinitesimal sphere surrounding the oscillating point dipole. However, it is straightforward to show that this is equal to Eq. (23). Now, we normalize this rate to the total radiative rate of an oscillating point dipole in a free space,

$$R_0 = \frac{|\vec{j}_0|^2\omega^2}{3c^3}, \tag{24}$$

and obtain the Purcell factor,

$$F_{\mathrm{P}} = \frac{R}{R_0}. \tag{25}$$

Similarly, the radiative part of Purcell factor can be found as a difference between the power flow through the top and the bottom interfaces of the complete structure,

$$F_{\mathrm{P}}^{\mathrm{rad}} = \frac{R^{\mathrm{rad}}}{R_0} = \frac{P_t - P_b}{R_0}. \tag{26}$$

For the scattering matrix calculation we use the Fourier modal method,[20,23] which has been improved by the formulation of the correct Fourier factorization rules[25] and adaptive spatial resolution,[26] as well as of matched coordinates for more complex metallic shapes.[27] In what follows, the results of these quantities will be presented employing 1633 spatial harmonics in the Fourier modal method with adaptive spatial resolution.[23,27]

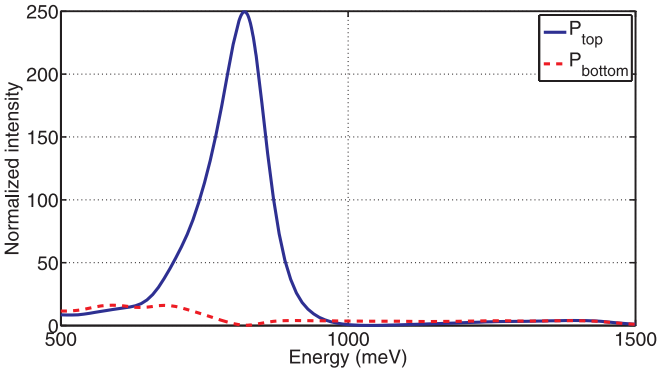

FIG. 3. (Color online) Calculated spectra of the emission in top (blue solid curve) and bottom (red dotted curve) directions of the oscillating point dipole (directed along x) coupled to the gold Yagi-Uda nanoantenna array. The intensity is normalized to the maximum radiation intensity of an equivalent dipole (with the same magnitude and the same frequency) in free space.

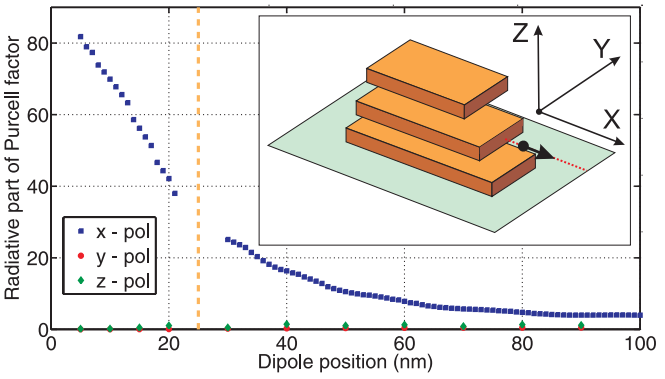

FIG. 5. (Color online) Calculated dependence of the radiative part of the Purcell factor F_P^{rad} on the horizontal distance between the dipole and the edge of the feed element for a x-, y-, and z-polarized dipole (squares, circles, and diamonds, respectively). The vertical dashed line marks the position exactly above the edge of the reflector. The geometry is explained in the inset: The x-polarized dipole is shown as a black dot with arrow, it is centered with respect to the feed element along y and z direction and shifted in x direction, along the dotted horizontal line.

III. NUMERICAL RESULTS AND DISCUSSION

The calculated emission spectra in top ($+z$) and bottom ($-z$) directions of the x-directed oscillating point dipole located inside the periodic array of gold Yagi-Uda nanoantennas are shown in Fig. 3. The dipole is placed on the horizontal symmetry axis along x direction at a distance of 5 nm to the edge of the feed element (see Fig. 1). Only one strong and narrow resonance occurs in the emission spectra in the top direction at the photon energy $\hbar\omega = 820$ meV ($\lambda = 1.5\,\mu$m). Its magnitude is about 250 times stronger than that of an equivalent dipole in free space and the FWHM is 107 meV. The emission to the bottom direction is significantly smaller. It even possesses a minimum at the plasmon resonance.

Figure 4 depicts the calculated radiation pattern of emission $P(\vartheta,\varphi)\,\vec{e}_r$ at the resonant photon energy $\hbar\omega = 820$ meV (where $\vec{e}_r$ is the radial unit vector of a spherical coordinate system centered in the point dipole position). The calculated radiative part of the Purcell factor according to the second part of Eq. (1) is as high as 80 (see also Fig. 5 below), which indicates very strong enhancement of the dipole emission by the feed element.

In spite of only one director employed in our Yagi-Uda antenna, the emission in top direction is highly directional. In order to characterize it, the angular directivity $D(\vartheta,\varphi)$ is calculated,[28] which indicates the part of the total emission radiated along the direction (ϑ, φ):

$$D(\vartheta,\varphi) = \frac{4\pi\, P(\vartheta,\varphi)}{\iint P(\vartheta,\varphi)d\Omega}. \tag{27}$$

Its maximum value $D^{max} = \max[D(\vartheta,\varphi)]$ is called directivity and indicates the antenna's ability to form a narrow beam. In the case of the radiation pattern of Fig. 4, $D^{max} = 4.7$; i.e., it exceeds the directivity of the dipole in free space ($D_0^{max} = 1.5$) by a factor of 3.1. In Ref. 3, the directivity of a single Yagi-Uda antenna with three directors has been calculated as 6.4, which is only 1.37 times larger than in our case with only a single

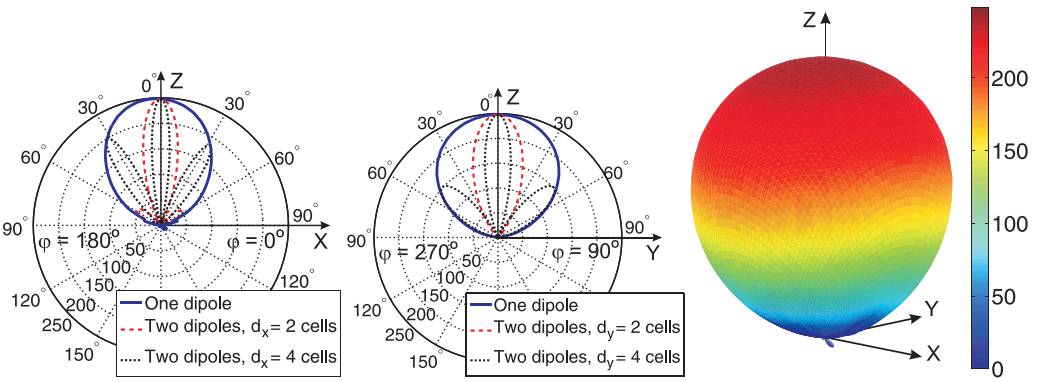

FIG. 4. (Color online) Calculated 2D polar diagrams (solid lines) of far-field emission in xz (left panel) and yz (central panel) planes, as well as the total 3D-directional diagram (right panel) for the x-oriented oscillating point dipole coupled to the gold Yagi-Uda nanoantenna array at resonant photon energy ($\hbar\omega = 820$ meV). The emission intensity is normalized to the maximum radiation intensity of the equivalent dipole (with the same magnitude and the same frequency) in free space and shown in the right panel as colored surface $P(\vartheta,\varphi)\,\vec{e}_r$. The dipole position is in the center-of-coordinates. Dashed lines in left and central panels show the scaled by a factor of 1/2 polar diagrams of $P_2(\vec{d},\vartheta,\varphi)$, the emission of a pair of synchronized dipoles separated by distance $\vec{d}$ (see explanation in the text).

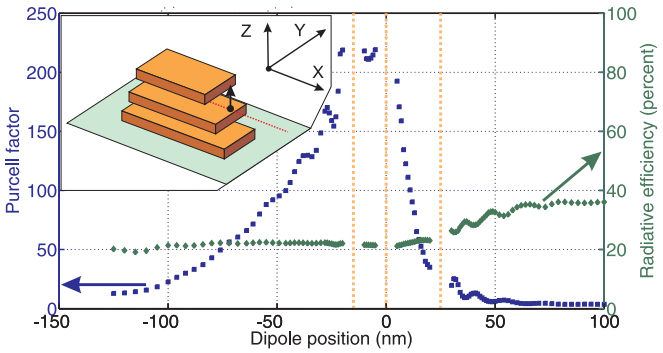

FIG. 6. (Color online) Calculated dependence of the Purcell factor F_P (squares) and the radiative efficiency η (diamonds) on the dipole position for a z-polarized dipole. The x coordinate of the dipole is changed from -125 to 100 nm (measured from the position of the edge of the feed element), while the y and z coordinate are fixed. The vertical dashed lines mark the positions exactly at the edges of the director, feed, and reflector elements. The geometry is explained in the inset: The z-polarized dipole is shown as a black dot with arrow; it lies 10 nm above the feed's upper horizontal surface, it is centered with respect to the feed element along y direction and shifted in x direction along the dotted horizontal line.

director. Furthermore, we can also increase the directivity using more than one dipole emitter coherently coupled to different antenna array elements, which is shown below.

It is also instructive to investigate the dependence of the emission enhancement on the dipole position and on the orientation of its dipole moment to the feed element. Figure 5 shows the calculated dependence of the radiative part of the Purcell factor F_P^{rad} with respect to the distance between the feed element and the dipole for x-, y-, and z-directed dipoles. The emission enhancement of the antenna array decreases with increasing distance. The strong polarization and distance dependence demonstrates the local nature of the antenna-dipole enhancement.

For the different distances indicated in the inset of Fig. 5, the emission is only significantly enhanced for the x-polarized dipole, which means that a plasmon mode with charges oscillating along x is excited in the system. Such a mode leads to a very strong enhancement of emission and determines the directional pattern. As the electromagnetic field near the edges of the feed element is known to have a dipolar character at the fundamental plasmon mode, it is not surprising that the radiation pattern (not shown here) of the z-polarized dipole displaced vertically by 10 nm above the edge of the feed element (see the black point in the inset of Fig. 6) nearly coincides with that of the x-polarized dipole 5 nm apart from the edge of the feed element (shown in Fig. 4). This effect has been demonstrated, for example, in Refs. 3,13, and 29. Unlike a z-polarized dipole in free space, the majority of the emission is directed along the dipole polarization (i.e., along the z axis). The magnitude, however, is about three times smaller than that of the x-oriented dipole.

At this point, let us discuss the results of the total Purcell factor F_P and the radiative efficiency η. The calculated results are shown in Fig. 6, where the dipole is placed 10 nm above the feed (i.e., in a homogeneous transparent glass). The Purcell factor is rather large and reaches the maximum of $F_P \approx 200$ when the dipole is located above the edge of the feed element. The radiative efficiency appears to be almost independent on the dipole's x coordinate and is about 20% when the emitter is above the feed element.

It should be mentioned that within the Fourier modal method we cannot calculate correctly the total Purcell factor as well as the radiative efficiency η if the dipole is inside a modulated layer (as, e.g., shown in Fig. 5). In this case, the discontinuous permittivity function of such a layer is described by a truncated Fourier expansion. As a result, due to the Gibbs phenomenon, the permittivity of the lossless surrounding of the lossy metal acquires a small imaginary part. On the other hand, the point dipole approximation fails if the dipole is placed inside a lossy material.

Finally, we would like to mention that the antenna array allows us to control the emission directivity further by using several emitting dipoles in different positions and controlling their phase difference of oscillations. Figure 4 shows the 2D polar diagrams (scaled by a factor of 0.5) of the emission of two phase-coherent dipoles positioned at neighboring antennas of the array at distance $\vec{d}$, proportional to integer numbers of periods (see dotted and dashed lines in the left and central panels). The emission intensity of the synchronized pair of dipoles normalized to the maximum emission intensity of two nonsynchronized dipoles is then simply

$$P_2(\vec{d},\vartheta,\varphi) = P(\vartheta,\varphi)[1+\cos(2\pi n(\vec{d}\cdot\vec{e}_r)/\lambda)], \qquad (28)$$

where $P(\vartheta,\varphi)$ is the directional pattern of a single dipole (solid line), and n is the refractive index of superstrate. Note that the polar diagrams P_2 of the synchronized dipoles demonstrate the effect of super-radiance: The Purcell factor of two synchronized closely positioned dipoles becomes twice as large than for the unsynchronized case. It hence becomes possible to increase the directivity using two coherently coupled emitting dipoles.

IV. CONCLUSION

We calculated for the first time that a gold Yagi-Uda nanoantenna array enhances and simultaneously redirects radiation of the oscillating point dipole. The dipole-nanoantenna enhancement depends very strongly on the oscillating frequency, dipole position, and orientation of its moment. It becomes possible to control the emission directivity further by using several coherently coupled emitting dipoles attached to different antennas in the array. This opens a road to manipulate the excited-state lifetime of a quantum emitter and to fabricate narrow beam nanoscale antennas in the optical range, which could be redirected just like an optical phased-array.

ACKNOWLEDGMENTS

We acknowledge support from BMBF (13N 9155, 13N 10146), DFG (FOR 557, FOR 730, GI 269/11-1), DFH/UFA, ANR Chair of Excellence Program, the Russian Academy of Sciences, the Russian Foundation for Basic Research, and the Dynasty Foundation.

[1]J. Li, A. Salandrino, and N. Engheta, Phys. Rev. B **76**, 245403 (2007).
[2]H. F. Hofmann, T. Kosako, and Y. Kadoya, New J. Phys. **9**, 217 (2007).
[3]T. H. Taminiau, F. D. Stefani, and N. F. van Hulst, Opt. Express **16**, 10858 (2008).
[4]T. Kosako, Y. Kadoya, and H. F. Hofmann, Nat. Photon. **4**, 312 (2010).
[5]J. Li, A. Salandrino, and N. Engheta, Phys. Rev. B **79**, 195104 (2009).
[6]A. Ahmadi and H. Mosallaei, Opt. Lett. **35**, 3706 (2010).
[7]H. Gersen, M. F. García-Parajó, L. Novotny, J. A. Veerman, L. Kuipers, and N. F. van Hulst, Phys. Rev. Lett. **85**, 5312 (2000).
[8]S. Kühn, G. Mori, M. Agio, and V. Sandoghdar, Mol. Phys. **106**, 893 (2008).
[9]A. Mohammadi, V. Sandoghdar, and M. Agio, New J. Phys. **10**, 105015 (2008).
[10]G. Sun, J. B. Khurgin, and R. A. Soref, J. Opt. Soc. Am. B **25**, 1748 (2008).
[11]G. Sun, J. B. Khurgin, and R. A. Soref, Appl. Phys. Lett. **94**, 101103 (2009).
[12]A. Kinkhabwala, Z. Yu, S. Fan, Y. Avlasevich, K. Müllen, and W. E. Moerner, Nat. Photon. **3**, 654 (2009).
[13]R. Esteban, T. V. Teperik, and J. J. Greffet, Phys. Rev. Lett. **104**, 026802 (2010).
[14]A. F. Koenderink, Nano Lett. **9**, 4228 (2009).
[15]W. L. Barnes, A. Dereux, and T. W. Ebbesen, Nature (London) **424**, 824 (2003).
[16]A. Polman, Science **322**, 868 (2008).
[17]E. M. Purcell, Phys. Rev. **69**, 681 (1946).
[18]G. W. Ford and W. O. Weber, Phys. Rep. **113**, 195 (1984).
[19]D. Dregely, R. Taubert, J. Dorfmüller, R. Vogelgesang, K. Kern, and H. Giessen, Nat. Comm. **2**, 267 (2011).
[20]D. M. Whittaker and I. S. Culshaw, Phys. Rev. B **60**, 2610 (1999).
[21]D. M. Whittaker, Opt. Lett. **25**, 779 (2000).
[22]H. Taniyama and M. Notomi, J. Appl. Phys. **103**, 083115 (2008).
[23]S. G. Tikhodeev, A. L. Yablonskii, E. A. Muljarov, N. A. Gippius, and T. Ishihara, Phys. Rev. B **66**, 045102 (2002).
[24]L. Li, J. Opt. Soc. Am. A **20**, 655 (2003).
[25]L. Li, J. Optics A **5**, 345 (2003).
[26]G. Granet and J.-P. Plumey, J. Optics A: Pure Appl. Optics **4**, S145 (2002).
[27]T. Weiss, G. Granet, N. A. Gippius, S. G. Tikhodeev, and H. Giessen, Opt. Express **17**, 8051 (2009).
[28]C. A. Balanis, *Antenna Theory*, 3rd edition (John Wiley & Sons, Hoboken, 2005).
[29]T. V. Teperik and A. Degiron, Phys. Rev. B **83**, 245408 (2011).